

Time-integrated nuclear resonant forward scattering of synchrotron radiation

R. Coussement, S. Cottenier, and C. L'abbé

*Instituut voor Kern-en Stralingsfysica, Physics Department, Catholic University of Leuven, Celestijnenlaan 200D,
B-3001 Heverlee, Belgium*

(Received 13 May 1996)

A formalism and computer simulations are presented to show that it is possible to use nuclear resonant forward scattering of synchrotron radiation without timing, allowing measurements to be made without modifying the electron-bunch operational mode of the synchrotron itself. [S0163-1829(96)04146-X]

INTRODUCTION

With the advent of the third generation of synchrotron-radiation machines, it became possible to use Mössbauer or resonant scattering in order to measure the hyperfine parameters of materials. The recent introduction of fast detectors allows the separation in time between the direct beam and the forward-scattered photons. This opens the way to also study polycrystalline samples by observation of the resonant nuclear scattering in the forward direction.¹ All such measurements can be described as broadband coherent excitation of an ensemble of nuclei by a short synchrotron-radiation pulse. The deexcitation of those coherently excited nuclei produces quantum beats which until now are observed as periodic oscillations in the time differential mode. In order to follow those quantum beats as a function of time, the delay between two adjacent excitation pulses coming from the synchrotron must be longer than the mean lifetime of the excited nuclear state. This special timing requirement can put restrictions on the use of synchrotron radiation for these kinds of measurements, as this operation mode reduces the possibilities for performing other experiments at the same time. In this paper we propose a time-integrated method in order to allow the use of the nuclear forward scattering in practically any operational mode of the storage ring and without limitations on the lifetime of the nucleus.

DESCRIPTION OF THE METHOD

In a time-integrated method the terms containing the quantum beats disappear because of the time integration, except when the quantum beat period is long compared to the nuclear lifetime. This happens when the two interfering transition frequencies are nearly the same. The idea of the method is to build in a variable frequency. This can be achieved easily by the introduction of a separate single-line scatterer. By moving only the single-line scatterer one can tune the transition frequency by using the Doppler shift. Each time the Doppler-tuned transition frequency crosses a hyperfine transition frequency of the sample under investigation the time-integrated quantum beat term will appear as a resonance peak. In this way the hyperfine splitting will appear if one registers the time-integrated counting as a function of the relative velocity between the reference single-line material and the investigated sample. This velocity spectrum will strongly resemble a Mössbauer absorption spectrum and

is easily interpretable. There are, however, essential differences because the interference of transition amplitudes are measured, and not the squares of the norm of the absorption amplitudes.

FORMALISM

In this method one measures the time-integrated transmission which contains (i) the photons that did not interact (the direct beam), as well as (ii) the forward-scattered ones in which we are interested. Because the scattered photons are delayed by typically the nuclear lifetime with respect to the direct beam, one can distinguish them experimentally from the scattered ones by means of a detector that recovers very fast after the flash of the direct photons. In previous experiments one measured the transmitted intensity as a function of the time after that flash. In the present proposal we do not need the time information, except that one must take care to eliminate the direct beam. The same formalism will allow us also to consider the use of a crossed polarizer and analyzer,^{2,3} in which case the elimination of the direct beam is not necessary.

In order to calculate the time-integrated forward-scattered intensity we can use the Parseval theorem in order to avoid the calculation in the time domain, the integration over time being replaced by an integration over the frequency (in the following the subscripts mean: in is incident, fs is forward scattered, tr is transmitted):

$$\begin{aligned} \int_0^{\infty} I_{fs}(t) dt &= \int_0^{\infty} E_{fs}(t) E_{fs}^*(t) dt \\ &= \frac{1}{2\pi} \int_{-\infty}^{+\infty} E_{fs}(\omega) E_{fs}^*(\omega) d\omega. \end{aligned} \quad (1)$$

The forward-scattered intensity is part of the transmitted intensity which also contains the photons that did not interact with the nuclei. The transmitted intensity is calculated in the Appendix. In a real experiment one avoids the overwhelming counting rate from the direct beam by cutting on the time axis. In order to subtract that direct from the transmitted beam we must work in the time rather than in the frequency domain which would require a Fourier transformation from frequency to time and a time-truncated transformation back to the frequency domain. We have however adopted avoiding that transformation, and we use the approximation of

previous papers⁴ in which is assumed that the duration of the excitation pulse is really so short, compared to the nuclear lifetime, that interference between incoming and forward-scattered amplitudes can be neglected.

$$E_{\text{tr}}(t) = E_{\text{in}}(t) + E_{\text{fs}}(t), \quad (2)$$

$$E_{\text{tr}}(\omega) = E_{\text{in}}(\omega) + E_{\text{fs}}(\omega).$$

The essential idea of this paper is to add a single-line reference scatterer. It introduces a supplementary scattering amplitude, which we will distinguish from the amplitudes from the sample by adding indexes. E_0 stands for the scattering amplitude of the reference sample with a resonance frequency ω_0 , while the other amplitudes from the sample to be studied are designated as E_j with resonance frequencies ω_j . As all these amplitudes are coherent we must add them:

$$E_{\text{fs}}(\omega) = E_0(\omega) + \sum_j E_j(\omega). \quad (3)$$

The total intensity then contains interference terms but they will vanish by the integration over time (or frequency) when the difference between the resonance frequencies is large compared to the natural or thickness-broadened linewidth. When two amplitudes have the same or nearly the same frequency the interference term contributes to the integrated intensities. This can be easily verified as well in the time domain as in the frequency domain. In the frequency domain we must integrate the product of two resonance amplitudes, which in first-order approximation becomes

$$\int_{-\infty}^{+\infty} \{E_0(\omega)E_j^*(\omega) + E_0^*(\omega)E_j(\omega)\} d\omega = \frac{C_j T_0 T_1}{(\omega_0 - \omega_j)^2 + \Gamma^2}. \quad (4)$$

In Eq. (4) C_j is a constant, T_0 and T_1 are the effective thicknesses of the reference sample and the sample under investigation. As the reference sample can be moved with respect to the sample under investigation, one can tune ω_0 by the Doppler shift as a function of the relative velocity, similar to a Mössbauer absorption spectrum. The integrated intensity will show a resonance of the type as in Eq. (4) at each velocity for which the Doppler-shifted reference frequency $\omega_0(1+v/c)$ crosses a frequency ω_j of the sample. The intensity of the resonance peak will be proportional to the product of the reference and the investigated scattering amplitudes and can be positive as well as negative, depending on the relative phase of the two scattering amplitudes. The width and shape of the resonance depend on the effective thicknesses of the samples. The position on the velocity scale gives the frequency shift with respect to the reference. We can thus conclude that it is possible to extract the same information as can be gained from the time-differential spectral method.

SIMULATIONS

In order to demonstrate and explore the time-integrated method we performed a number of computer simulations for a double absorber containing natural iron. On the second—moving—absorber we imposed no interactions, giving a

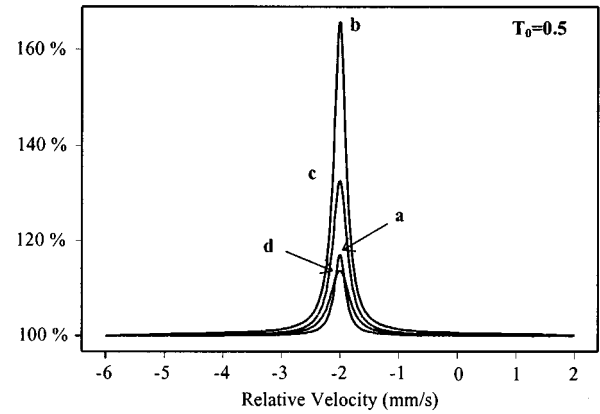


FIG. 1. Single-line spectra normalized to the baseline intensity (a) $T_1=0.05$, (b) $T_1=0.5$, (c) $T_1=1.5$, (d) $T_1=3.5$.

single-line environment for the ^{57}Fe probe nuclei. Its effective thickness is denoted by T_0 . The first—stationary—absorber (effective thickness T_1) was subject to (i) no interactions, (ii) a magnetic interaction, and (iii) a quadrupole interaction. The moving absorber was given an isomer shift of 2 mm/s with respect to the first one. In cases (ii) and (iii), we present results in two modes: with and without crossed polarization filters. In the latter case the hyperfine axis was chosen at an angle of 45° with respect to the polarizer and analyzer. The incoming beam was assumed to be fully linearly polarized. Its intensity was taken constant in frequency and time at 1 photon per second per natural linewidth of ^{57}Fe . With this normalization, the actual number of counts per second in the time-integrated spectra can be calculated from the values on the Y axes multiplied by the actual intensity of the synchrotron and divided by the number of velocity channels.

Stationary single-line absorber

As can be seen in Fig. 1, the width and the height of the resonance peaks grow when the effective thickness of one of the absorbers becomes larger. The intensity of the baseline itself is strongly dependent on the effective thicknesses (Fig. 2). Simulations show that the peak-to-baseline intensity ratio

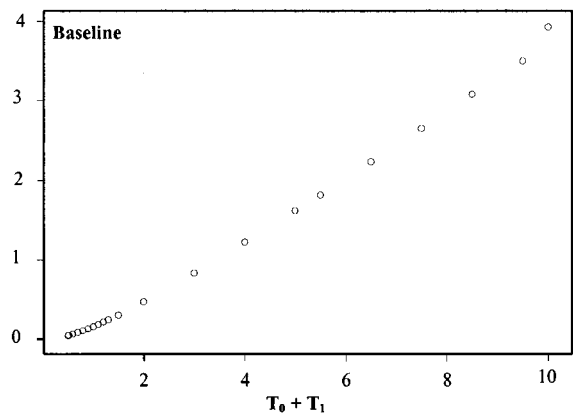


FIG. 2. Baseline intensity for single-line spectra as a function of $T_0 + T_1$.

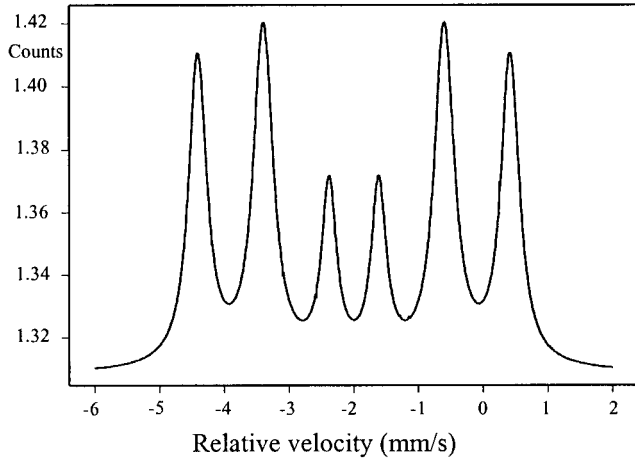


FIG. 3. $\mathbf{B}=15$ T, $T_0=1$, $T_1=5$, without crossed polarizer and analyzer.

becomes maximum when the two effective thicknesses are equal.

These effects can be understood by considering that the intensity of the forward scattered photons is the square of the norm of the total amplitude as given in Eq. (3):

$$I_{fs}(\omega) = \underbrace{|E_0|^2 + \sum_j |E_j|^2}_{\text{baseline}} + \underbrace{\sum_j \{E_0 E_j^* + E_0^* E_j\}}_{\text{peak}}. \quad (5)$$

It will thus contain two types of terms: the cross terms or interference terms and the square terms or partial intensity terms. From Eq. (4) it can be seen that in first-order approximation (=for small thicknesses) the cross terms are proportional to the product of the effective thicknesses. The baseline contains the sum of the partial intensity terms, which explains its sensitivity to the effective thickness. This also explains why the maximum value for the peak-to-baseline ratio is found when the effective thickness of the reference sample is equal to the one of the sample under investigation.

Stationary magnetic absorber

We assume a magnetic field of 15 T perpendicular to the synchrotron beam and applied only on the stationary absorber. Its effective thickness T_1 was taken to be 5. In order to more or less optimize the number of counts in the time-integrated spectrum, T_0 was given a value of 1. The polarization plane of the beam was taken at 45° with respect to the hyperfine axis.

In Fig. 3, a Mössbauer-like spectrum appears with a resonance peak whenever the single-line frequency of the moving absorber crosses a transition frequency of the magnetically split stationary absorber. However the intensities of the peaks are different from those in a Mössbauer spectrum because one observes interferences between the single-line amplitude and the amplitudes of the sample under study. This is caused by the fact that with synchrotron radiation all transitions are excited simultaneously and hence interferences between these transitions are possible. At resonance there are more counts than elsewhere, because there the total effective

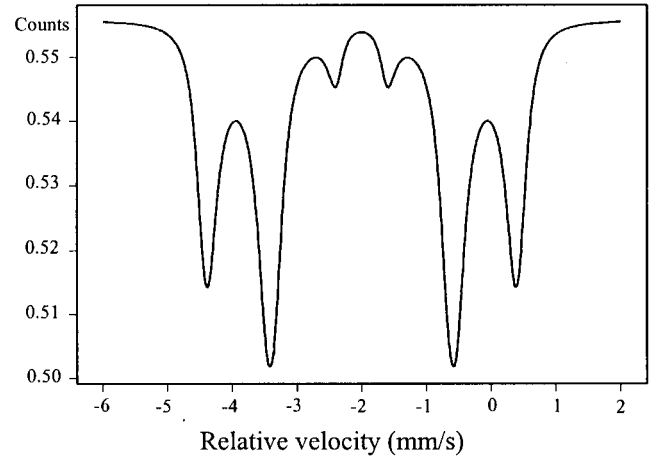


FIG. 4. $\mathbf{B}=15$ T, $T_0=1.5$, $T_1=5$, with polarizer and analyzer.

thickness is the sum of T_0 and T_1 (and not either T_0 or T_1). As the forward scattered intensity is a positive function of T_0+T_1 (Fig. 2), we see indeed an enhancement.

Figure 4 shows the result for the same absorbers, but now with a crossed polarizer analyzer equipment. We see a different spectrum having absorption peaks. As explained above, the results of the first type of experiments are based on the interference of the scattering amplitudes from the reference and investigated samples. However, in the following we will explain why in the cross polarizer case, these interferences cannot occur and hence these results have to be explained differently. As the scattering on the single-line reference does not change the polarization, its amplitude remains x linearly polarized and cannot interfere with the y polarized amplitude of the sample which is the only component allowed to the detector by the analyzer. Moreover x and y components are orthogonal and could not interfere. What happens is that the polarizer analyzer selects the resonance or near resonance frequencies of the investigated sample as far as the linear polarization has changed from x to y . The intensities of the transmitted radiation is thus peaked around the resonance frequencies similar as from a Mössbauer source. The effect of the reference sample is to partially absorb those y linear polarized and peaked intensities when its frequency is properly tuned by the Doppler shift.

We remark that the single-line absorber can be placed everywhere in the beam. It appears clearly from the formalism in the Appendix. The effect on the wave when passing through the single-line scatterer/absorber is a transformation of the amplitude and this transformation can be expressed by a matrix proportional to an identity matrix. This matrix commutes with all other matrices which express the transformation of the field amplitude when the photon propagates through the different components of the experimental setup.

Stationary absorber with electric-field gradient

Figures 5 and 6 show the time-integrated spectra for a single crystal with an electric-field gradient (EFG) of 10^{22} V/m² perpendicular to the beam, T_0 being 1.5 and T_1 equal to 5.

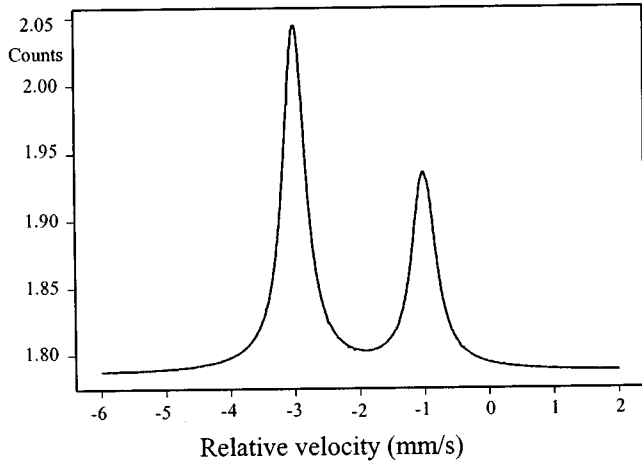


FIG. 5. $EFG=10^{22}$ V/m², $T_0=1.5$, $T_1=5$, without polarizer and analyzer.

The same comments for the magnetic spectra apply here. The surprise in Fig. 6 is the appearance of a hole burning in the resonance peak of the $\pm 1/2 \rightarrow \pm 1/2$ transition. Such a hole burning is the result of an interference between a negative single- and the corresponding double-scattering amplitude.

DISCUSSION

We distinguish two different procedures in the use of the time-integrated method: the interference with a variable reference frequency and the crossed polarization method.

The use of the interference of a variable reference frequency for the detection or measurement of an unknown one is a standard procedure in telecommunications and other measurement procedures and is called *heterodyne detection*. The present application differs from most others by the detection in a time-integrated mode. One of the authors has already used that procedure in a nuclear level crossing experiment with the aim to compare an unknown quadrupole frequency to a variable Zeeman frequency.⁴

The variant with the crossed polarization devices will make any timing requirement totally unnecessary and eventual background can be suppressed by the use of a detector that permits energy selection. It has the disadvantage that it does not work for a single-line spectrum and also not for powders with random orientation of the hyperfine axes.

The key achievement of the measurement procedure is the possibility to lessen the timing requirements of the storage ring in such a way that the measurements can be performed in a parasite mode: the synchrotron operation being optimized for other users.

The second important opportunity is the possibility to study long-living Mössbauer isotopes, for example ¹⁸¹Ta with a lifetime of 6 μ s. When the crossed polarizer analyzer method is used it becomes possible to study short-living isomers. The only limit is that the hyperfine splitting must be larger than the natural linewidth. It may thus be possible to extent the number of hyperfine probes by this method.

There are a number of other advantages with respect to the time-differential method. The obtained velocity spectra

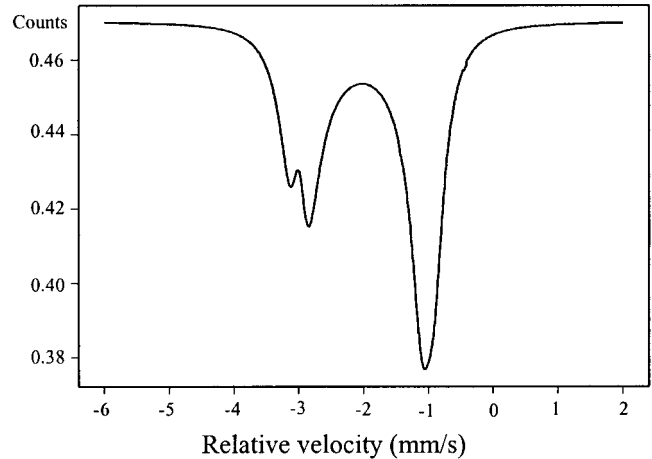


FIG. 6. $EFG=10^{22}$ V/m², $T_0=1.5$, $T_1=5$, with polarizer and analyzer.

can be interpreted practically “on line” like a Mössbauer spectrum. It will be a non-negligible advantage when experiments are performed with strong input intensity with the aim of rapid and systematic studies, especially when on-line decisions may be required. The method will also offer a big advantage when the investigated sample contains different components with a distribution of hyperfine fields. In the time-differential mode, the number of beat frequencies may become unreasonably large in order to allow for an easy analysis of the time spectrum, because, in principle, each frequency belonging to one field component can interfere with each frequency of the other field component.

The interference method also has the advantage that the minimum linewidth is only one and not two times the natural linewidth as in conventional source Mössbauer spectroscopy. This is also true for the time-differential method because both methods, at least in first order, are based on the interference of two single-scattering amplitudes. On the other hand, the procedure with the crossed polarization device has a minimum linewidth of two times the natural linewidth because the effect is the product of two probabilities; the probability that the photons are coherently forward scattered by the hyperfine split sample and the probability that they are absorbed incoherently by the single-line absorber.

In the past we have used the combination of an electric quadrupole interaction with a magnetic dipole interaction as a function of the magnetic field. We studied the change in the anisotropy of the nuclear radiation when the magnetic field is swept through a crossing field and we demonstrated theoretically and experimentally that the radiation anisotropy displays resonances. In the case of coherent resonant forward scattering we must observe a similar resonant behavior. Indeed, at the crossing field two interfering transition frequencies become equal, the beat frequency is zero and consequently at and near that field the interference term does not cancel by time integration. As a function of the magnetic field we will thus find a resonance, a level crossing resonance. The applicability of these types of resonances is rather limited by the conditions that one needs two collinear interaction axes and that the quadrupole splitting must be larger

than the natural linewidth. However an interesting variant of the crossing idea is the pure magnetic zero-field crossing. It happens when only a magnetic field is applied which can be changed from high to zero field. With high field we mean that the magnetic splitting must be larger than the natural linewidth. It must be possible to observe carefully the phase transition from magnetic to paramagnetic by measuring as a function of temperature and one may be able to deduce the critical exponents with high accuracy if the temperature can be finely tuned and stabilized.

Another idea emerging from this study is the possibility to measure the change of effective thicknesses as a function of parameters such as temperature or pressure in an elegant and efficient way. According to Fig. 2 and its explanation, it is sufficient to put only the sample in the beam and store the time-integrated countrate as a function of the variable parameter. As such a measurement requires very little equipment—no timing, no velocity drive, no reference sample—its application to measure the Debye temperature of a material must be easy and quick.

ACKNOWLEDGMENTS

The authors would like to thank Professor G. Hoy of the Old Dominion University in Norfolk, Virginia and Professor J. Odeurs and Dr. G. Neyens, both of the Catholic University

of Leuven, Belgium for their helpful suggestions and discussions. S.C. would like to thank the NFWO (National Fund for Scientific Research, Belgium) for financial support.

APPENDIX: CALCULATION OF THE TRANSMITTED AMPLITUDE E_{tr}

In the frequency domain the transmitted amplitudes for right- and left-handed circular polarization through a single scatterer are calculated from the set of differential equations:

$$\begin{bmatrix} \frac{dE_{tr}^+(\omega)}{dz} \\ \frac{dE_{tr}^-(\omega)}{dz} \end{bmatrix} = -i\lambda n \begin{bmatrix} f^{++}(\omega) & f^{-+}(\omega) \\ f^{+-}(\omega) & f^{--}(\omega) \end{bmatrix} \begin{bmatrix} E_i^+(\omega) \\ E_i^-(\omega) \end{bmatrix}, \quad (A1)$$

in which E^+ and E^- stands for the amplitude of photons with right- and left-handed circular polarization, respectively. The summed density of all isotopes of the scattering element is called n . The forward-scattering amplitudes f_j for a nucleus with N transitions are given as in Ref. 5, including the effective thickness, the dependence on the angle β between the hyperfine field, and the beam direction, and the Clebsch-Gordan coefficients:

$$f^{\sigma\sigma'}(\omega) = -\frac{k}{8\pi} \sigma_0 f_{LM} \chi \frac{3}{2} \sum_{j=1}^N \frac{\Gamma/2}{\omega - \omega_j - i\Gamma/2} C^2(j_e, 1, j_g; m_e, \Delta m_j, m_g) D_{\Delta m_j, \sigma}^1(\alpha, \beta, \gamma) D_{\Delta m_j, \sigma'}^{1*}(\alpha, \beta, \gamma). \quad (A2)$$

Further symbols are the cross section σ_0 , the Lamb-Mössbauer factor f_{LM} , the isotopic abundance χ , and the natural linewidth Γ . σ and σ' are the circular polarizations of the incoming and outgoing photons.

In Eq. (A1) we distinguish the diagonal elements of the f matrix which are related to forward-scattering processes in which the circular polarization is not changed. The nondi-

agonal ones stand for the processes in which the circular polarization changes. They vanish when the hyperfine fields are axially symmetric with respect to the propagation axis of the photon but not in the usual geometry with the hyperfine fields perpendicularly or randomly oriented.

The solution for that set of coupled linear differential equations gives the transmitted amplitude as a function of the incoming one:

$$\begin{bmatrix} E_{tr}^+(z, \omega) \\ E_{tr}^-(z, \omega) \end{bmatrix} = S_I \begin{bmatrix} E_{in}^+(z=0, \omega) \\ E_{in}^-(z=0, \omega) \end{bmatrix},$$

$$S_I = \begin{bmatrix} A & B \\ C & D \end{bmatrix} = \begin{bmatrix} \left\{ e^{\nu z} \frac{\sqrt{+a-d}}{2\sqrt{}} + e^{\mu z} \frac{\sqrt{-a+d}}{2\sqrt{}} \right\} & \left\{ \frac{b}{\sqrt{}} (e^{\nu z} - e^{\mu z}) \right\} \\ \left\{ \frac{c}{\sqrt{}} (e^{\nu z} - e^{\mu z}) \right\} & \left\{ e^{\nu z} \frac{\sqrt{-a+d}}{2\sqrt{}} + e^{\mu z} \frac{\sqrt{+a-d}}{2\sqrt{}} \right\} \end{bmatrix}. \quad (A3)$$

The symbols used for shortness are explained below:

$$\begin{aligned}
 a &= i\lambda n \sum_{j=1}^N f_j^{++}(\omega), \\
 b &\leftrightarrow f^{-+} \quad c \leftrightarrow f^{+-} \quad d \leftrightarrow f^{--}, \\
 \sqrt{} &= \sqrt{(a-d)^2 + 4cb}, \\
 \mu &= \frac{-(a+d) + \sqrt{}}{2}, \\
 \nu &= \frac{-(a+d) - \sqrt{}}{2}.
 \end{aligned} \tag{A4}$$

To obtain the transmitted amplitude after a second absorber, the results from Eq. (A3) are inserted into these equa-

tions again as the new E_{in} , with appropriate values for a , b , c , and d which are absorber dependent. The transformation of the transmitted field can be expressed as a transformation matrix S_I , the matrix elements contain all the parameters, known and unknown, of the scatterer. When two different scatterers are used the total transformation is given as the product of the two transformation matrices. The right sequence must be respected as the two matrices may not commute in some cases.

The matrix for a single-line scatterer simplifies [because for a single-line $\sqrt{}=0$, S_I has to be treated using de l'Hopital rules to find the correct limits in Eqs. (A3)] because of the symmetries between the diagonal and nondiagonal elements of the scattering matrix in Eq. (A1). By intuition one can expect that a single-line sample does not distinguish between different circular polarizations because of its forward backward symmetry and therefore we must expect the matrix S_I to become scalar for this case. This is proved as follows:

For a single-line absorber/scatterer it follows from Eqs. (A1) and (A2) that

$$f^{\sigma\sigma'}(\omega) = -\frac{k}{8\pi} \sigma_0 f_{\text{LM}\chi} \frac{3}{2} \frac{\Gamma/2}{\omega - \omega_0 - i\Gamma/2} \sum_{\Delta m_j} \sum_{m_e} \sum_{m_g} C^2(j_e, 1, j_g; m_e, \Delta m_j, m_g) D_{\Delta m_j, \sigma}^1(\alpha, \beta, \gamma) D_{\Delta m_j, \sigma'}^{1*}(\alpha, \beta, \gamma). \tag{A5}$$

Because of the relations

$$\begin{aligned}
 \sum_{m_e, m_g} C^2(j_e, 1, j_g; m_e, \Delta m_j, m_g) &= 1, \\
 \sum_{\Delta m_j} D_{\Delta m_j, \sigma}^1(\alpha, \beta, \gamma) D_{\Delta m_j, \sigma'}^{1*}(\alpha, \beta, \gamma) &= \delta_{\sigma, \sigma'}, \tag{A6}
 \end{aligned}$$

we find that

$$f^{+-} = f^{-+} = 0 \quad \text{and} \quad f^{++} = f^{--}. \tag{A7}$$

The transformation matrix S_I for this case becomes

$$S_I = e^{-a_{\text{ref}} d_{\text{ref}}} \begin{bmatrix} 1 & 0 \\ 0 & 1 \end{bmatrix} = S_R. \tag{A8}$$

This matrix we call S_R (from *Reference material*), while the matrix describing the impact of the *Investigated material* remains to be called S_I . The symbol d_{ref} is used for the thickness z of this reference material, a_{ref} is a new name for the previous symbol a (“ a ” conserves its previous meaning for the investigated material).

In these expressions we have preferred to use the circular rather than the linear polarization representation of the photon, because it is easier to express the scattering amplitudes. As the synchrotron radiation is strongly linearly polarized and as furthermore linear polarizers and analyzers are used we will need to transform from one representation to the other one. The transformation from the linear to circular polarization representation is given by the matrix equation:

$$\begin{bmatrix} E_x \\ E_y \end{bmatrix} = \underbrace{\frac{1}{\sqrt{2}} \begin{bmatrix} -1 & +1 \\ i & i \end{bmatrix}}_{\text{U}} \begin{bmatrix} E^+ \\ E^- \end{bmatrix}. \tag{A9}$$

If we describe the impact of an X polarizer and Y analyzer in the linear basis by matrices too,

$$P_X = \begin{bmatrix} 1 & 0 \\ 0 & 0 \end{bmatrix}, \quad P_Y = \begin{bmatrix} 0 & 0 \\ 0 & 1 \end{bmatrix}, \tag{A10}$$

we can easily describe the transmission of a synchrotron beam through consecutively an X polarizer, the investigated sample, the single-line reference sample, and finally through a Y analyzer by this matrix equation:

$$\begin{aligned} \begin{bmatrix} E_x^{\text{out}} \\ E_y^{\text{out}} \end{bmatrix} &= P_Y U S_R S_I U^{-1} P_X \begin{bmatrix} E_x^{\text{in}} \\ E_y^{\text{in}} \end{bmatrix} \\ &= E_x^{\text{in}} \frac{i e^{-a_{\text{ref}} d_{\text{ref}}}}{2} (-A + B - C + D) \begin{bmatrix} 0 \\ 1 \end{bmatrix}. \end{aligned} \quad (\text{A11})$$

From Eq. (A11) we easily see that if a single-line sample is investigated ($A = D$, $B = C = 0$) no outgoing radiation is detected.

When the polarizer/analyzer setup is not used and the synchrotron beam is fed directly into the investigated sample this equation becomes

$$\begin{aligned} \begin{bmatrix} E_x^{\text{out}} \\ E_y^{\text{out}} \end{bmatrix} &= U S_R S_I U^{-1} \begin{bmatrix} E_x^{\text{in}} \\ E_y^{\text{in}} \end{bmatrix} \\ &= \frac{e^{-a_{\text{ref}} d_{\text{ref}}}}{2} \begin{bmatrix} A - B - C + D & i(A + B - C - D) \\ i(-A + B - C + D) & A + B + C + D \end{bmatrix} \\ &\quad \times \begin{bmatrix} E_x^{\text{in}} \\ E_y^{\text{in}} \end{bmatrix}. \end{aligned} \quad (\text{A12})$$

We can easily derive again that the resulting matrix reduces to a scalar one and no transformation of polarization occurs when the investigated sample is of a single-line type.

¹J. B. Hastings, D. P. Siddons, U. van Bürck, R. Hollatz, and U. Bergmann, *Phys. Rev. Lett.* **66**, 770 (1991).

²D. P. Siddons *et al.*, *Nucl. Instrum. Methods Phys. Res. Sect. B* **103**, 371 (1995).

³T. S. Toellner, E. E. Alp, W. Sturhahn, T. M. Mooney, X. Zhang, M. Ando, Y. Yoda, and S. Kikuta, *Appl. Phys. Lett.* **67**, 1993 (1995).

⁴S. Shibuya, M. Fujioka, N. Kawamura, A. Matsumoto, S. Hayashibe, Y. Kimura, T. Ishimatsu, R. Coussement, M. Rots, L. Hermans, and P. Put, *Hyperfine Interact.* **14**, 315 (1983).

⁵G. V. Smirnov, *Proceedings of the 10th International Conference on Hyperfine Interactions* [*Hyperfine Interact.* **97/98**, 551 (1996)].